4. Beam Optics

4.1 Introduction

The usefulness of a synchrotron radiation source may be judged by an experimenter primarily in terms of how many photons per second, area and solid angle can be directed onto the sample. High brilliance[1] is a figure of merit for this aspect, which can be achieved by using insertion devices.

The experimental needs, in the Middle East region, ask (in addition to high brilliance) for high photon energy range. Increasing the photon critical energy[2] (with conventional bending magnets and wigglers) by going from 1 to 2 GeV in electron beam energy, made a convenient solution for this requirement.

$$\varepsilon_c(keV) = 0.665 B(T) E^2 (GeV) \qquad (4.1)$$

Low emittance is a figure of merit for 3rd generation machines. With the limited beam current, going to smaller beam emittance increases the brilliance[1], which makes this characteristic one of our principle goals in designing the ring lattice.

Low emittance is of our interest, and increasing the number of bending magnets (BM) is the most effective way to get it.

$$\varepsilon_x \propto E^2 . F(\mu_s, lattice) / J_x . N_{BM}^3 \qquad (4.2)$$

In SESAME, this aim was faced by limitted number of BMs and limited ring circumference. Using BMs with field gradient (n > 0) increases the horizontal damping-partition number J_x from 1 up to 2 at the maximum, which means decreasing emittance up to by factor of 2 at the maximum[1]. Also minimizing the dispersion in the dipoles (BMs) by using dispersion distribution method[1], participates in emittance decreasing:

$$\varepsilon_x = C_q \gamma^2 \langle H \rangle_{mag} / J_x \rho \qquad (4.3)$$

where:

$$\langle H \rangle_{mag} = \int (\gamma_x \eta^2 + 2\alpha_x \eta \eta' + \beta_x \eta'^2) ds / 2\pi\rho \qquad (4.4)$$

$$J_x = 1 - I_4 / I_2 \ , \ I_4 = \int_{BM} (1-2n)\eta / \rho^2 ds \ , \ I_2 = \int_{BM} 1/\rho^2 ds \ , \ C_q = 3.84.10^{-13} m.rad$$

We see also that increasing the bending radius of bending magnets ρ_0 decreases emittance, but this (for certain number of BMs) increases the length of the BM which, in turn, increases the ring circumference.

To get the desired optics we use the quadrupole magnets with enough number of families and convenient strengths and arrangements. A high machine-flexibility is important to control the optics easily even for any future modifications, and it is directly proportional to the number of quadrupole families, taking into account the limitations on the quadrupoles number and ring circumference length.

Chromaticity[3], which is caused by the quadrupoles must be corrected to keep the beam in the storage ring for reasonable lifetime. This is done by 2 families of sextupole magnets put in dispersion sections, with convenient locations.

Nonlinearities and the unwanted effects of these sextupoles[3] can be minimized by other sextupoles distributed in a suitable locations and families number.

In general, the best solution for a lattice is the one which achieves all the optical, geometrical, and economical advantages we want, but usually we get some on the expense of the others, so a compromise must be made to get the optimum solution.

4.2 The Lattice

In order to get as small emittance as possible, with the limited dipoles (BMs) number, we used dispersion distribution lattice with gradient in dipoles.

High photon energy radiation with high brilliance is of our interest, so we aimed to offer enough number of straight sections to accommodate the needed insertion devices. So, an 8-fold symmetric ring with 16 straight sections of enough length was a good solution for our lattice which is shown in the optical function diagram Figure (4.1), followed by its structure Table (4.1).

We see from Equation (4.4) that a small β_x in the dipoles participates in decreasing the emittance, which is shown by Figure (4.1).

Because of the gradient in the dipoles, it was sufficient to use just 3 families of quadrupoles to get the desired optics, which saved 2 vertical-focusing quadrupoles in each superperiod.

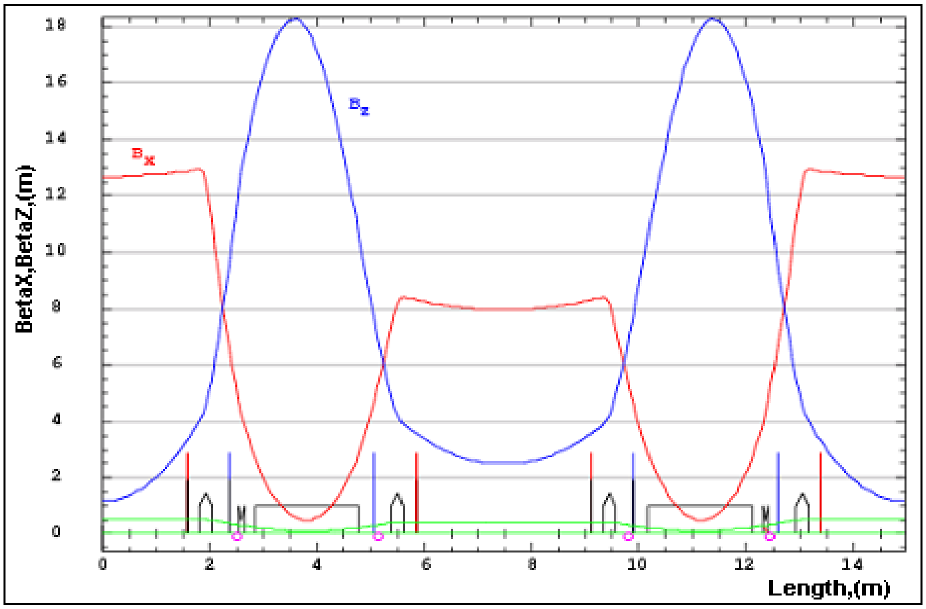

Figure 4.1: Optical functions of SESAME lattice, the green line represents dispersion. Horizontal and vertical correctors are represented by red and blue respectively inside the sextupoles. BPM's are represented by the pink circles.

In order to obtain low vertical beam dimension and to minimize the undesirable effects of the insertion devices on optics, we use 8 sections with low β_z (= 1.14 m) to accommodate wigglers, and the others for accommodating undulators.

The ratio ($\sum$ straight section length) / circumference is a figure of merit for storage rings in the world. This lattice design shows that we are at a high level of this criterion. SESAME storage ring parameters are shown in Table (4.2).

A good working point, in a stable area on the tune diagram is a crucial indication of the machine stability. The tune diagram of SESAME lattice Figure (4.2), shows the working-point position from different types of resonances

Table 4.1: The elements of the lattice and the structre of one superperiod. The total storage ring is composed of 8 superperiods

Name code	Element	Length (m)	$\rho(m)$	$k(m^{-2})$	$m(m^{-3})$	$s(m)$
1	D1	1.5				1.5
2	S1	0.15			4.31382	1.65
3	D2	0.15				1.8
4	Q1	0.23		2.9343		2.03
5	D3	0.25				2.28
6	S2	0.15			-5.767	2.43
7	D4	0.1				2.53
8	Q2	0.11		-2.8506		2.64
9	D5	0.2				2.84
10	rB	1.9406	4.9416	-0.341		4.78
11	D6	0.2				4.98
12	S3	0.15			-21.338	5.13
13	D7	0.25				5.38
14	Q3	0.23		2.74526		5.61
15	D8	0.15				5.76
16	S4	0.15			15.0206	5.91
17	D9	1.559				7.469
18	D9	1.559				9.028
19	S4	0.15			15.0206	9.178
20	D8	0.15				9.328
21	Q3	0.23		2.74526		9.558
22	D7	0.25				9.808
23	S3	0.15			-21.338	9.958
24	D6	0.2				10.158
25	rB	1.9406	4.9416	-0.341		12.099
26	D5	0.2				12.299
27	Q2	0.11		-2.8506		12.409
28	D4	0.1				12.509
29	S2	0.15			-5.767	12.659
30	D3	0.25				12.909
31	Q1	0.23		2.9343		13.139
32	D2	0.15				13.289
33	S1	0.15			4.31382	13.439
34	D1	1.5				14.939

Table 4.2: SESAME storage ring parameters

Parameter	**Unit**	**Value**
General Parameters		
Energy	(GeV)	2.0
Beam current	(mA)	400
Circumference	(m)	125
Natural emittance	(nm rad)	16.8
Coupling	(%)	2.0
Horizontal emittance	(nmrad)	16.5
Vertical emittance	(nmrad)	0.3302
Horizontal working point		7.27
Vertical working point		5.22
Momentum compaction factor		0.0079
Relative energy spread	(%)	0.090
Chromaticity (horizontal)		-13.26
Chromaticity (vertical)		-14.9
Machine Functions		
Horizontal beta functions		
Wiggler / bending / undulator	(m/rad)	7.94/0.482/12.7
Vertical beta functions		
Wiggler / bending / undulator	(m/rad)	2.47/17.9/1.14
Disperson function		
Wiggler / bending / undulator	(m)	0.40/0.112/0.52
Beam Sizes and Cross Sections		
Horizontal beam size		
Wiggler / bending / undulator	(μm)	510 / 134 / 656
Vertical beam size		
Wiggler / bending / undulator	(μm)	28.5 / 70.9 / 19.4
Cross section		
Wiggler / bending / undulator	(mm^2)	0.091/0.060/0.080
R.F-System		
Energy loss (bending) per turn	(KeV)	286.4
Energy loss (per wiggler) per turn	(KeV)	25.7
R.F.-frequency	(MHz)	499.654
Harmonic number		200
R.F.-power	(kW)	250
Number of cavities		2
Beam power (2 wigglers)	(kW)	135.1
Shunt impedance per cavity	(MΩ)	3.4
R.F.-cavity voltage	(kV)	553
Overvoltage factor		3.3
Energy acceptance	(%)	1.2
Bunch length	(mm)	12.0

Having 4 families of sextupoles in SESAME lattice was sufficient for minimizing chromaticity and optimizing nonlinear effects of sextupoles.

Optimizing nonlinearities makes the tune shift with amplitude as smooth as possible; to keep the working points of particles with different amplitudes from falling into fatal resonances, see Figure (4.3).

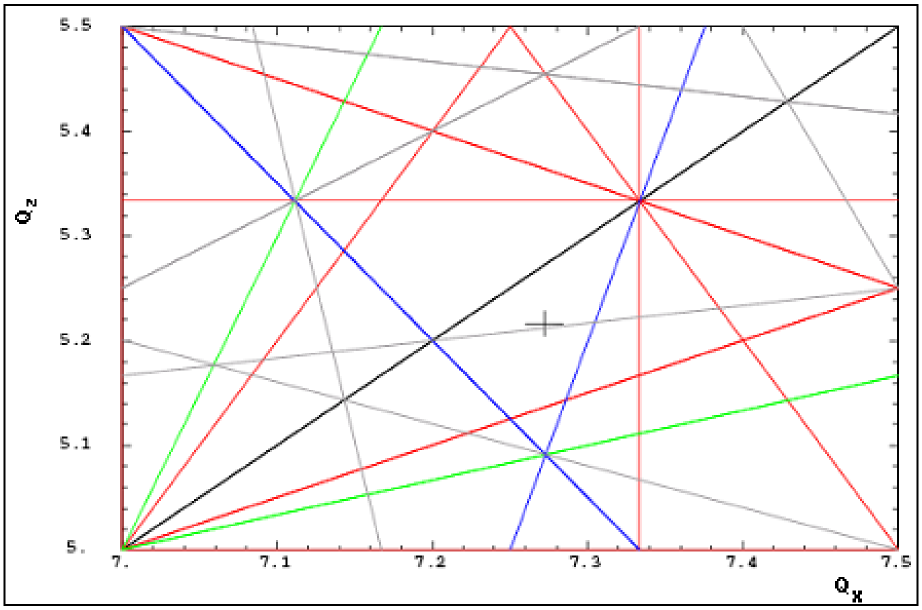

Figure 4.2: Tune diagram. This graph shows all the 2nd order (in black) and 3rd order (in red) resonances as well as the systematic 4th order (in green), 5th order (in blue) and 7th order (in grey) resonances.

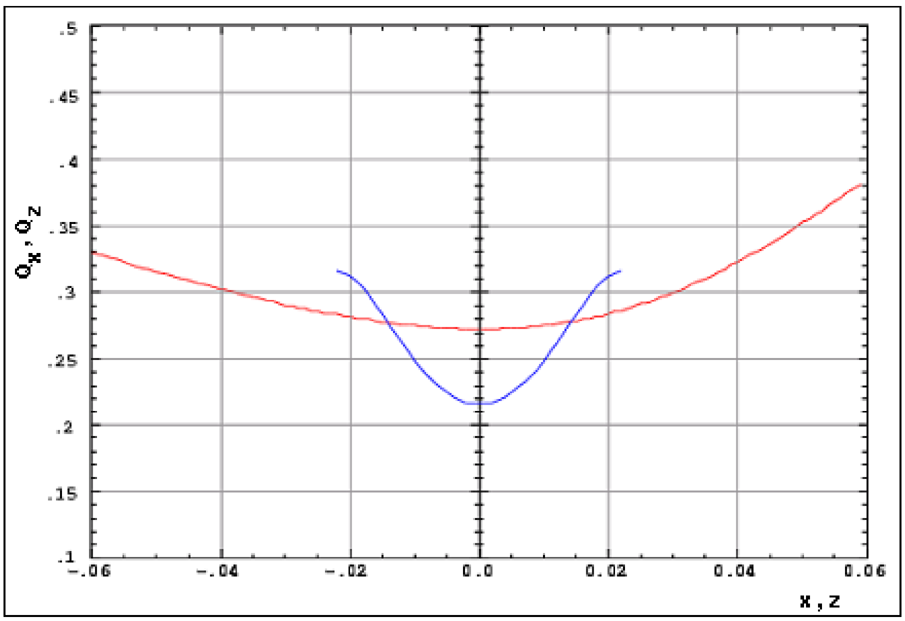

Figure 4.3: Tune shift with betatron amplitude. Horizontal (in red) tune integer part = 7, vertical (in blue) tune integer part = 5

This increases the stable area available for the beam in x,z plane (dynamic aperture) which must be at least the same size as the vacuum chamber (physical aperture). Particle tracking for 1000 revolutions at the middle of high horizontal-beta, low vertical-beta section is shown in Figure (4.4).

Getting enough dynamic aperture provides, in turn, more lifetime for the beam and more efficient injection.

A high energy acceptance of the ring is necessary to increase the beam lifetime, by enhancing Touschek one[4].

A smooth tune shift with *ΔE/E* keeps the working points of off-momentum particles, from hitting dangerous resonances up to enough energy acceptance, see Figure (4.5).

Dynamic apertures of particles with *ΔE/E = 2%* and *ΔE/E = -2%* in the real space of vacuum chamber are shown in Figure (4.6). Oscillation of these particles around different closed orbits must be taken into account.

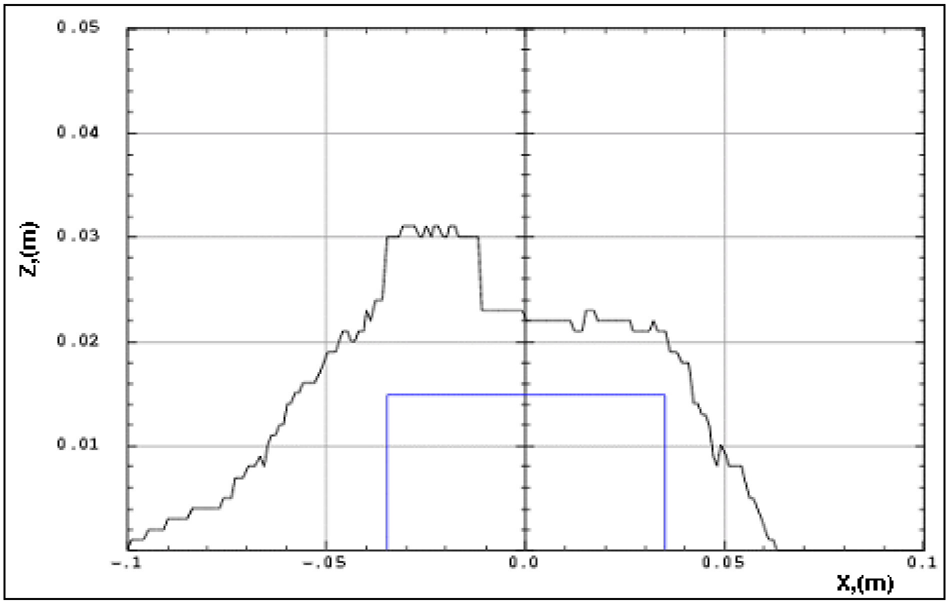

Figure 4.4: Dynamic aperture (in black) for on-momentum particle, calculated for 1000 turns. Physical aperture is shown in blue.

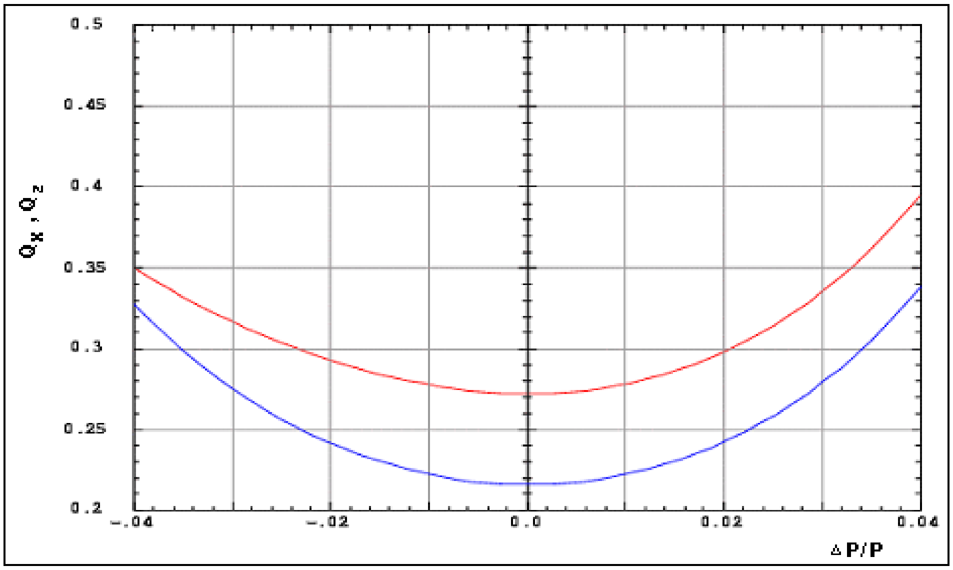

Figure 4.5: Horizontal (in red) and vertical (in blue) tune shifts with energy deviation

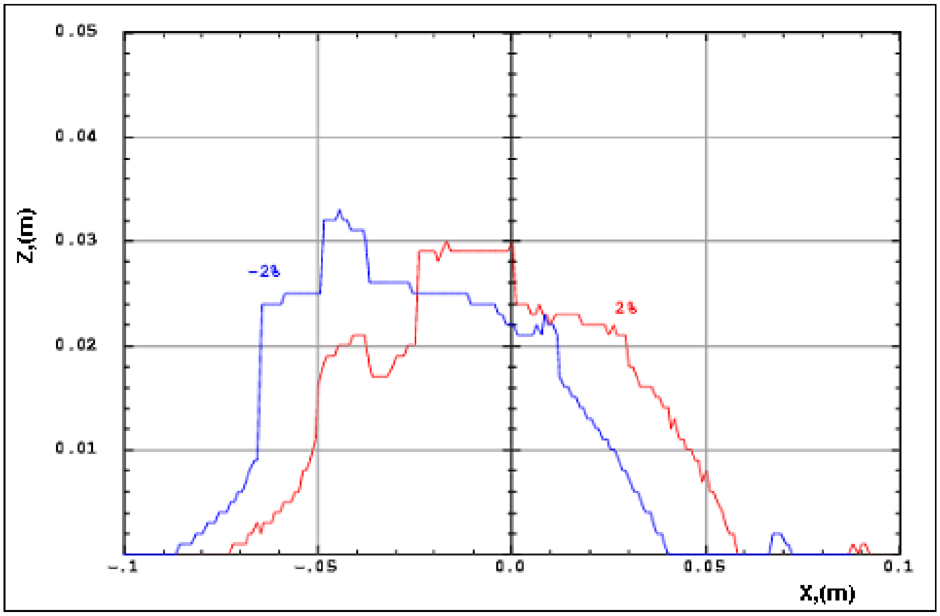

Figure 4.6: Dynamic aperture for off-momentum particles of: 2% (in red) and – 2% (in blue)

4.3 Choice of Working Point

To avoid instabilities, a loss and a blow up of the beam the working point (Q_x and Q_y) must be far away from a resonance line. The resonance lines are given by:

$$m \cdot Q_x + n \cdot Q_y = k \cdot P \qquad (4.5)$$

m, n and k are integers, P is the periodicity of the machine. With a high periodicity the amount of resonance lines decreases in general. According to this, the periodicity should be as high as possible. The resonance lines and their driving terms are given in the following Table (4.3). Figure (4.7) gives the resonance line diagram with the working point and an indication of the lines. In Table (4.4) the resonance lines around the working point with their order and some remarks to their seriousness are summarized.

According to Table (4.4) and Figure (4.7) only the lines Q4, Q6 and Q9 could be dangerous. All lines are 3^{rd} order ones; Q4 and Q6 are driven by normal sextupoles; Q9 is driven by a skewed sextupole. These three resonance lines determine the behavior of the beam. The limits of Figure (4.3) and (4.5) are in the range of the Q_x =7.33 and Q_y = 5.33. Both values are given by the resonance lines Q6 and Q9. According to this analysis the working point in the horizontal direction should perhaps moved to Q_x = 7.22

Table 4.3: Resonance lines and their driving forces

Order of Multipole	Number of poles	Resonance Lines	Resonance lines	Number of Lines
		Normal	skewed	
N=1 (integer)	2	$Q_x = k$	$Qy = k$	2
N=2 (half integer)	4	$2Q_x = k$ $2Q_y = k$	$Q_x \pm Q_y = k$	4
N=3 (third integer)	6	$3Q_x = k$ $Q_x \pm 2Q_y = k$	$3Q_y = k$ $2Q_x \pm Q_y = k$	6
N=4 (fourth integer)	8	$4Q_x = k$ $2Q_x \pm 2Q_y=k$ $4Q_y = k$	$3Q_x \pm Qy = k$ $Q_x \pm 3Q_y = k$	8
N=5 (fifth integer)	10	$5Q_x = k$ $3Q_x \pm 2Q_y = k$ $Q_x \pm 4Q_y = k$	$5Q_y = k$ $4Q_x \pm Q_y = k$ $2Q_x \pm 3Q_y = k$	10
N=6 (sixth integer)	12	$6Q_x = k$ $4Q_x \pm 2Q_y = k$ $2Q_x \pm 4Q_y = k$ $6Q_y = k$	$5Q_x \pm Q_y = k$ $3Q_x \pm 3Q_y = k$ $Q_x \pm 5Q_y = k$	12

Table 4.4: Resonance lines around the working point (see Figure (4.7)). Nor. =normal, Ske. = Skewed, Med.-dist. = medium distance

Name	Equation	Order	Remark	Gravity
Q1	$3Q_x – Q_y =2*8$	4th	Ske. octup.	Far away, no dangerous
Q2	$2Q_x – Q_y = 9$	3rd	Ske. sextup.	Far away, no dangerous
Q3	$Q_x – Q_y = 2$	2nd	Ske. quadrup.	Med,-dist., no dangerous
Q4	$Q_x – 2Q_y = -3$	3rd	Nor. sextup.	Near by, could bedangerous
Q5	$Q_x – 3Q_y = -8$	4th	Ske. octup.	Far away, no dangerous
Q6	$3Q_x = 22$	3rd	Nor. sextup.	Med.-dist., could be dangerous
Q7	$4Q_x – Q_y =3*8$	5th	Ske. deducop.	Med.-dist., no dangerous
Q8	$Q_x – 6Q_y =3*8$	7th		Near by, no dangerous
Q9	$3Q_y = 2*8$	3rd	Ske. sextup.	Med.-dist., could be dangerous
Q10	$5Q_y = 26$	5th	Ske. deducop	Near by, no dangerous
Q11	$2Q_x + Q_y = 20$	3rd	Ske. sextup.	Far away, no dangerous
Q12	$3Q_x + 2Q_y =4*8$	5th	Nor. deducop.	Med.-dist., no dangerous

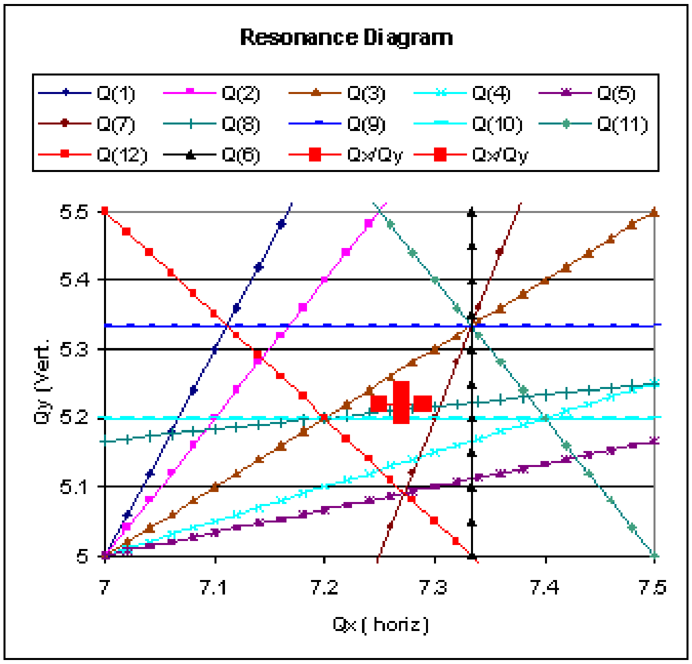

Figure 4.7: Working point within the resonance diagram. The order of the lines are given in the Table (4.4).

4.4 Effect of Insertion Devices on SESAME Optics

Using insertion devices[5] in synchrotron radiation facilities, provides radiation with enhanced features compared to that from bending magnets: higher photon energies, higher flux and brightness, and different polarization characteristics.

Insertion devices, in general, have undesirable effects on beam optics. They cause tune shift, beta beating especially in vertical plane. They affect emittance and energy spread.

A preliminary study on the effect of an ideal wiggler[B=2 T, L = 2.24 m, λ = 0.08 m] on the beam optics of SESAME lattice, revealed that in spite of a small extra increase in emittance, putting these wigglers in the sections of low β_z (= 1.14m) causes less total optical distortions-represented by less tune shift and beta beating- than in sections of high β_z (= 2.47m). So keeping the low-β_z sections for wigglers and the high-β_z sections for undulators gives a good distribution for the IDs in the ring.

In relation with our ring symmetry; using even number of wigglers gives more symmetric distorted optical functions and less beta beating. Using 8 wigglers gives complete symmetric optical functions with no beta beating, and even enhances the dynamic aperture over the original one, with small increase in emittance. Figures (4.8) - (4.11) show these results.

Global compensation for the tune shift was the best solution, which saves power supplies compared to local or any other compensation, and doesn't affect the flexibility of the lattice, which can be reduced in case of local compensation because of the presence of one family of quadrupoles in the undulator sections.

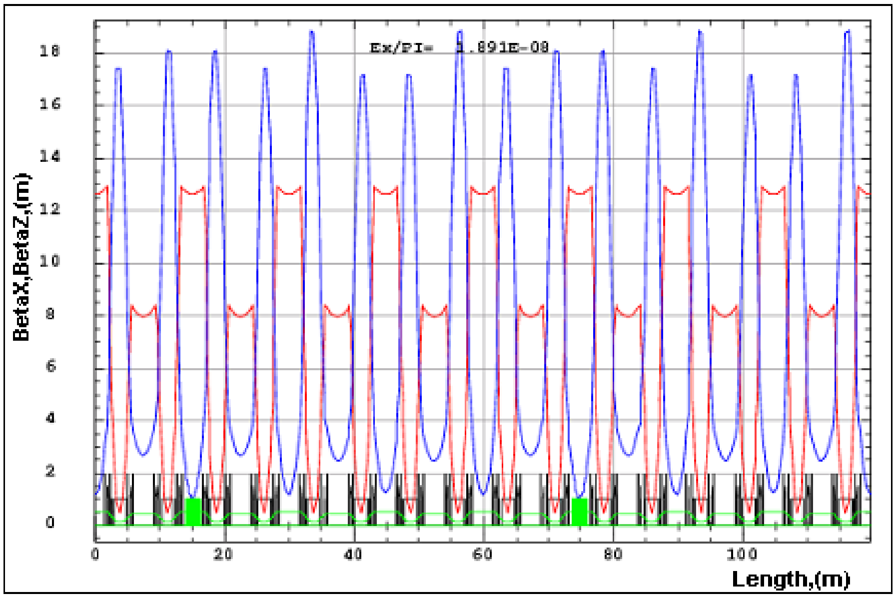

Figure 4.8: Effect of 2 wigglers on optics, after global compensation. Beta beating = 8%; Q_x = 2.272, Q_z = 5.216

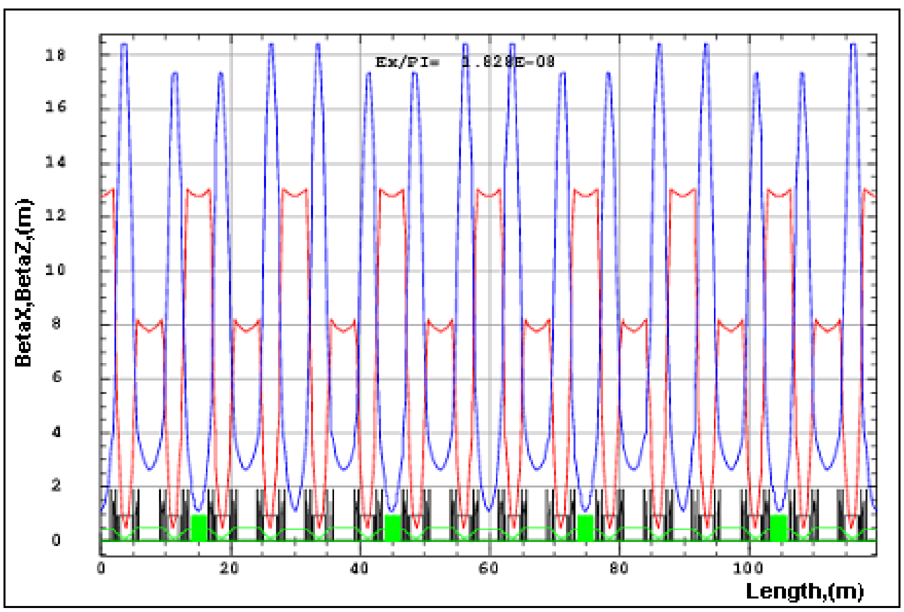

Figure 4.9: Effect of 4 wigglers on optics, after global compensation. Beta beating = 6.5% ; Q_x = 7.272, Q_z = 5.216

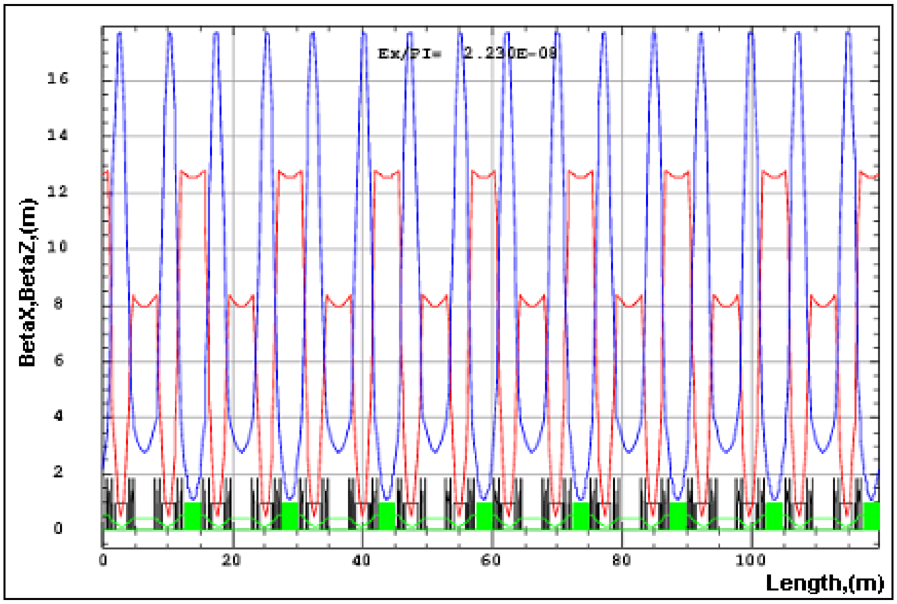

Figure 4.10: Effect of 8 wigglers on optics, after global compensation. Beta beating = 0% ; Q_x = 7.272, Q_z = 5.216

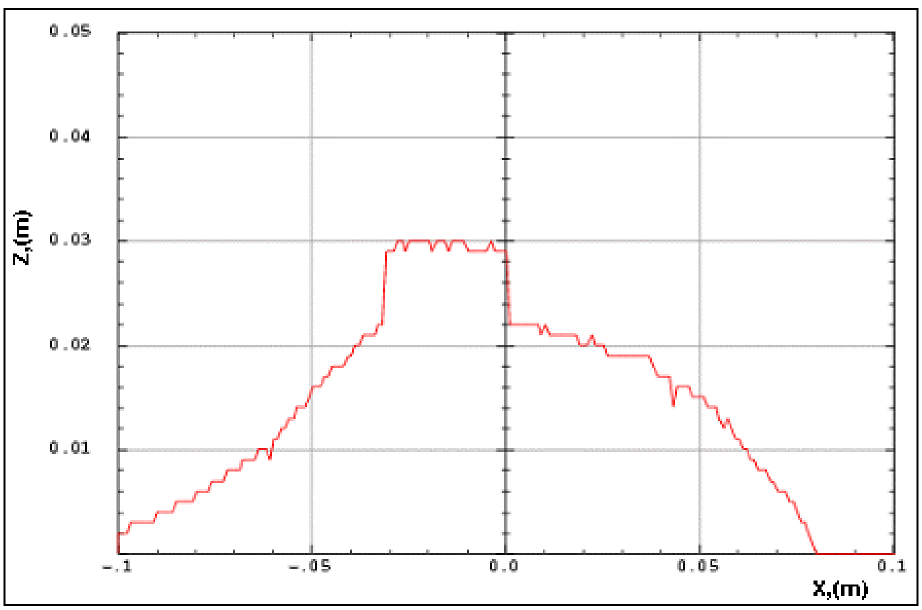

Figure 4.11: Effect of 8 wigglers on dynamic aperture after global compensation, calculated for 1000 turns.

4.5 Closed Orbit correction

Real machines contain different types of errors produced by misalignment of ring devices, magnetic field errors and several external error sources, which can be averaged statistically.

These errors cause distortion and instability for the beam closed orbit [6], which consumes the physical aperture, reduces the dynamic aperture, changes the optics and, in case of variation with time, disturbs emittance and brilliance. So it must be corrected.

Closed orbit correction[7] can be done by using corrector magnets and beam position monitors.

Closed orbit distortion is caused mainly by dipolar kicks produced by some residual errors, mainly: misalignments of dipoles, field errors in dipoles and displacement of quadrupoles.

By introducing 3σ of the errors shown in Table (4.5) to SESAME ring, and tracking over 100 different samples, the maximum horizontal closed orbit distortion was in the straight sections with a value between +8 and -8 mm as shown in Figure (4.12), while in vertical plane, the maximum distortion was in the dipoles as shown in Figure (4.13), with a value between +20 and -20 mm.

Table 4.5

Magnet type	**Type of error**	**RMS value of error**
Dipole	Field error	$5 \cdot 10^{-4}$
	Displacement dx = dz = ds	0.2 mm
	Rotation around s ($d\varphi_s$)	0.2 mrad
Quadrupole	Displacement dx = dz	0.1 mm

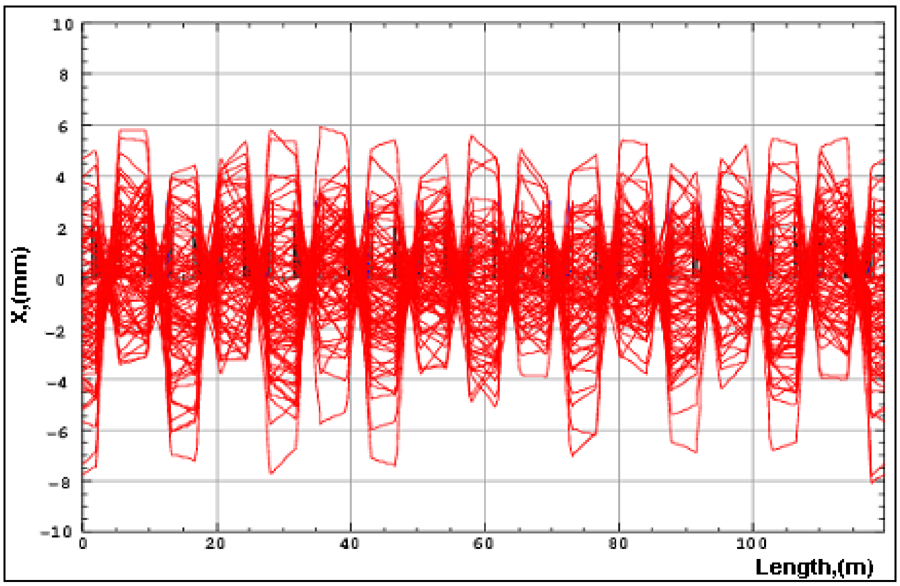

Figure 4.12: Simulation of uncorrected horizontal closed orbit distortion, done for 100 samples

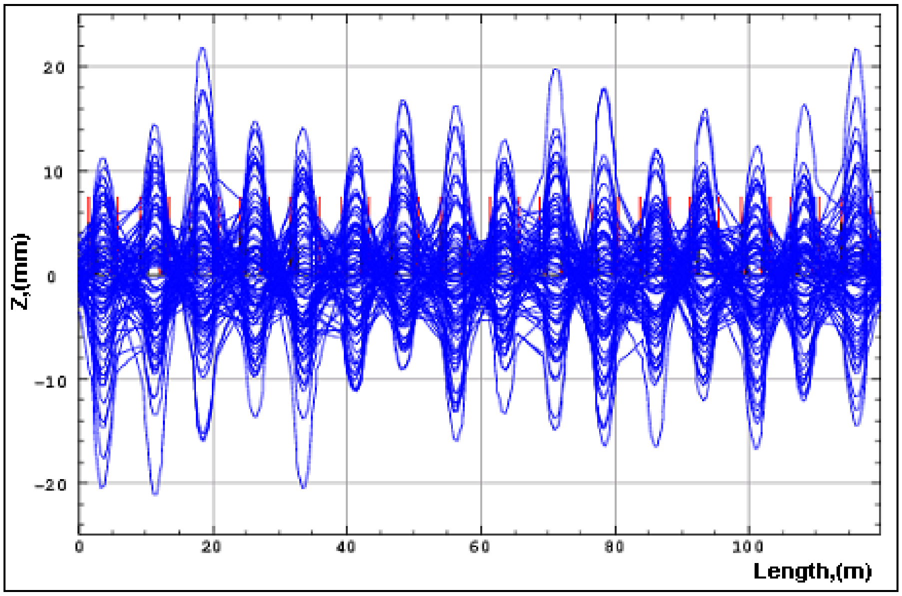

Figure 4.13: Uncorrected vertical closed orbit distortion

By using 32 beam position monitors together with 32 horizontal and 32 vertical correctors put inside the sextupoles as shown in Figure (4.1), the closed orbit distortion can be corrected to a maximum distortion value of ± 0.2 mm in horizontal and vertical planes as shown in Figures (4.14) and (4.15).

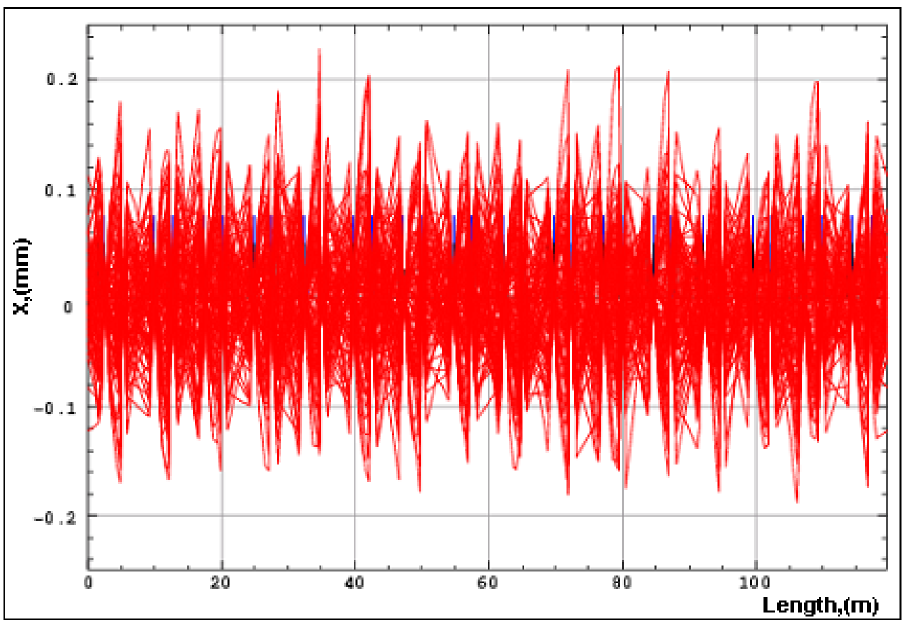

Figure 4.14: Corrected horizontal closed orbit distortion

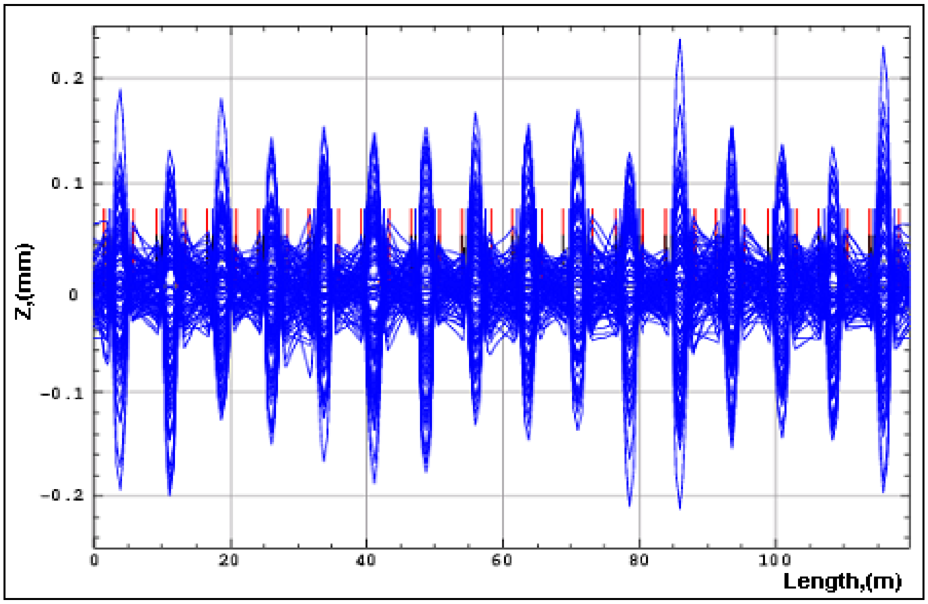

Figure 4.15: Corrected vertical closed orbit distortion

4.6 Coupling

The coupling [8] between the vertical and horizontal emittance is determined by the misalignment of the magnets in the horizontal or vertical plane. With a perfect alignment the coupling would be zero and so the vertical emittance too.

The alignment of the magnets at SESAME will be made with the same precision as for other light sources. Hence for SESAME we will have roughly the same coupling factor.

At existing 3rd generation light sources the coupling factor is around 1 %. At the ESRF for example the coupling factor is about 0.1 %, which is a very small number. At the beginning we take a coupling factor of 2 % for SESAME, which is very conservative.

4.7 Specifications of the Magnets

The optical properties of SESAME lattice, which determine the beam behavior, are results of a specific arrangement of different magnetic elements with specific parameters. These magnetic elements with their principal parameters, are mentioned in the following subsections.

4.7.1 The Bending Magnets

All these magnets have the same parameters and are in the same family. Their parameters are displayed in Table (4.6):

Table 4.6

Parameter	Unit	Value
Length	m	1.9406
Bending Angle	radian	0.3927
Bending Radius	m	4.9416
Magnetic Field Gradient	T/m	-2.27

4.7.2 The Quadrupole Magnets

These magnets are divided into 3 families (groups), all families has the same properties. Table (4.7) shows the length and the magnetic field gradient of these magnets:

Table 4.7

Family	Q1	Q2	Q3
Length (m)	0.23	0.11	0.23
Magnetic Field Gradient (T /m)	19.575	-19.0165	18.3139

4.7.3 The Sextupole Magnets

Theses magnets are divided into 4 families, all families has the same properties which are shown in Table (4.8).

Table 4.8

Family	S1	S2	S3	S4
Length (m)	0.15	0.15	0.15	0.15
Magnetic Strength (m^{-3})	43.1382	-57.6711	-213.3813	150.206

4.7.4 The Corrector Magnets

The corrector magnets in SESAME lattice will be put as coils inside the sextupoles, and they have the same length as the sextupoles.

Closed orbit distortion is corrected by two types of correctors: horizontal for the horizontal distortion correction and vertical for the vertical one. Their length and maximum kick strength are shown in Table (4.9).

Table 4.9

Type of Corrector	Horizontal	Vertical
Length (m)	0.15	0.15
Maximum Kick (radian)	$1.66*10^{-4}$	$1.1*10^{-4}$

4.8 Lifetime of the Stored Beam

4.8.1 Introduction

The requirements of the users are a good stability, a small cross section and a long lifetime of the beam. The wishes about a small cross section and a long lifetime of the beam are contradictionary, because the Touschek lifetime goes with the cross section of the beam. The lifetime of the stored beam is determined by the cross section of the different interaction processes of the stored beam with the atoms and molecules within the vacuum chamber. These processes are: 1) Elastic scattering of the beam at the nucleus (Coulomb scattering) 2) Inelastic scattering at the nucleus (Bremsstrahlung) 3) Elastic scattering at the bounded electrons of the atoms and molecules 4) Inelastic scattering at the bounded electrons of the atoms and molecules and 5) Touschek lifetime.

The lifetime τ according to an exchange process is given by:

$$\tau = \frac{1}{\sigma \cdot n \cdot c} \qquad (4.6)$$

where:

σ: cross section of the exchange process
n: particle density within the vacuum chamber
c: speed of light ($=2.9989*10^8$ m/s)
n_z: number of atoms per molecule

The pressure in the vacuum chamber gives the density n:

$$n = 3.22 \cdot 10^{22} (m^{-3}) \cdot (p/Torr) \cdot n_z \qquad (4.7)$$

Inserting c and n in Equation (4.6), the lifetime is given by:

$$\tau = \frac{1.04 \cdot 10^{-18} s \cdot cm^2}{\sigma \cdot (p/nTorr) \cdot n_z} = \frac{2.88 \cdot 10^{-22} hours}{(\sigma/cm^2) \cdot (p/nTorr) \cdot n_z} \qquad (4.8)$$

The calculation of the cross sections of the different exchange processes will be performed in the next paragraphs.

4.8.2 Elastic Scattering at the Nucleus (Coulomb Scattering)

The cross section for this exchange process is:

$$\sigma_{Coul} = \frac{2}{\gamma^2} \cdot \pi r_e^2 Z^2 \cdot \left\{ \frac{\langle \beta_x \rangle \beta_{x,0}}{A_x^2} + \frac{\langle \beta_y \rangle \beta_{y,0}}{A_y^2} \right\} \qquad (4.9)$$

Where:

- r_e: classical electron radius (=2.82*10-^{13} cm)
- Z: charge of the nucleus
- γ: normalised or reduced energy (= 1957*(E/GeV))
- A: aperture
- $\beta_{i,0}$: beta function, where the aperture has a minimum
- β_i: average beta function

With the insertion of π and the classical electron radius in the Equation (4.13) the cross section is given by:

$$\sigma_{Coul} = 2.50 \cdot 10^{-25} cm^2 \cdot \frac{2Z^2}{\gamma^2} \left\{ \frac{\langle \beta_x \rangle \beta_{x,0}}{A_x^2} + \frac{\langle \beta_y \rangle \beta_{y,0}}{A_y^2} \right\} \qquad (4.10)$$

With the Equation (4,10) the life time for the Coulomb scattering is:

$$\tau_{Coul} = 2.21 \cdot 10^9 hours \cdot \frac{(E/GeV)^2}{Z^2 (p/nTorr) n_z} \left\{ \frac{\langle \beta_x \rangle \beta_{x,0}}{A_x^2} + \frac{\langle \beta_y \rangle \beta_{y,0}}{A_y^2} \right\}^{-1} \qquad (4.11)$$

With the data: $(\beta_x)_{aver}$ = 7.5 m/rad, $\beta_{x,0}$= 12.5 m/rad, $(\beta_y)_{aver}$ = 7.57 m/rad, $\beta_{y,0}$ = 18.87 m/rad, A_x = 50 mm*mrad, A_y = 8.55 mm*mrad, Z = 7, n_z = 2 and p= 2 nTorr, the lifetime is:

$$\tau_{Coul} = 22.6 hours$$

The Coulomb scattering lifetime is proportional to the square of the energy. Changing the energy from 2 to 2.5 GeV, would increase the lifetime by a factor 1.56. With an energy of 1 GeV, the lifetime would decrease to 5.6 hours.

In order to reach for SESAME a lifetime more than 40 hours, the pressure should be smaller than 1 n Torr.

4.8.3 Inelastic Scattering at the Nucleus (Bremsstrahlung)

The cross section for the inelastic scattering at the nucleus is:

$$\sigma_{Brems} = \frac{16}{\pi \cdot 411} \cdot \pi r_e^2 Z^2 \cdot \ln\left(\frac{183}{Z^{1/3}}\right) \cdot \left\{ \ln\left(\frac{1}{(\delta E / E)_{rf}} - \frac{5}{8} \right) \right\} \qquad (4.12)$$

With the insertion of all constants in Equation (4.8) the cross section becomes:

$$\sigma_{Brems} = 3.10 \cdot 10^{-27} cm^2 \cdot Z^2 \cdot \ln \frac{183}{Z^{1/3}} \cdot \left\{ \ln\left(\frac{1}{(\delta E / E)_{rf}} - \frac{5}{8} \right) \right\} \qquad (4.13)$$

Inserting this in Equation (4.8) the lifetime for the Bremsstrahlung is given by:

$$\tau_{Brems} = \frac{9.29 \cdot 10^4 \, hours}{(p / nTorr) n_z Z^2 \ln \frac{183}{Z^{1/3}}} \cdot \left\{ \ln\left(\frac{1}{(\delta E / E)_{rf}} - \frac{5}{8} \right) \right\}^{-1} \qquad (4.14)$$

with Z=7 the lifetime will be:

$$\tau_{Brems} = \frac{415.6 hours}{(p / nTorr) n_z} \cdot \left\{ \ln\left(\frac{1}{(\delta E / E)_{rf}} - \frac{5}{8} \right) \right\}^{-1} \qquad (4.15)$$

With an energy acceptance of 1.2 % for the RF-system, $n_z = 2$ and a pressure of 2 nTorr the lifetime for the Bremsstrahlung is:

$$\tau_{Brems} = 27.4 \text{ hours}$$

By changing the energy acceptance to 2.4 % the lifetime will increase to 33.47 hours. To influence the lifetime of the Bremsstrahlung very much, it is only possible to decrease the pressure. With a pressure of 1 nTorr the corresponding lifetime would be:

45.8 hours

4.8.4 Elastic Scattering at the Bounded Electrons

The electrons of the stored beam can be scattered at the bounded electrons of the atoms and molecules. During this process energy from the stored electrons are being transferred to the bounded electrons. If this energy is larger than the energy acceptance of the RF-system, the scattered electrons will be lost. The cross section for the elastic scattering at the electrons of the atoms and molecules are given by:

$$\sigma_{Coul}(e) = \frac{2}{\gamma} \cdot \pi r_e^2 Z \cdot \frac{1}{(\delta E / E)_{rf}} \qquad (4.16)$$

$$\sigma_{Coul}(e) = 3.181 \cdot 10^{-25} cm^2 \frac{Z}{\gamma} \cdot \frac{1}{(\delta E / E)_{rf}} \qquad (4.17)$$

The insertion of (4.17) in Equation (4.8) gives the corresponding life time:

$$\tau_{Coul}(e) = 1.128 \cdot 10^4 \, hours \frac{(E / GeV)(\varepsilon_{rf} / \%)}{Z(p / nTorr) n_z} \qquad (4.18)$$

For an energy of 2 GeV, a pressure of 2 nTorr, Z = 7, n_z = 2 and an energy acceptance of 1.2 %, the lifetime will be:

$$\tau_{Coul}(e) = 967 \text{ hours} \qquad (4.19)$$

This is a very long lifetime, which has not to be considered in the future. $\tau_{Coul}(e)$ goes with the energy and also for a 1 GeV machine the lifetime of 484 hours is very long.

4.8.5 Inelastic Scattering at the Bounded Electrons

This is the same process as described in Section 4.8.3, but the stored electrons will be scattered at the electrons of the atoms or molecules. The corresponding cross section is:

$$\sigma_{Brems}(e) = \frac{16}{\pi \cdot 411} \cdot \pi r_e^2 Z \cdot \left\{ \ln\left(\frac{2.5\gamma}{(\delta E / E)_{rf}} \right) - 1.4 \right\} \cdot \left\{ \ln\left(\frac{1}{(\delta e / E)_{rf}} \right) - \frac{5}{8} \right\} \qquad (4.20)$$

By inserting the constants the cross section will be:

$$\sigma_{Brems}(e) = 3.10 \cdot 10^{-27} cm^2 Z \cdot \left\{ \ln\left(\frac{2.5\gamma}{(\delta E / E)_{rf}} \right) - 1.4 \right\} \cdot \left\{ \ln\left(\frac{1}{(\delta e / E)_{rf}} \right) - \frac{5}{8} \right\} \qquad (4.21)$$

The corresponding lifetime is:

$$\tau_{Brems}(e) = \frac{9.30 \cdot 10^4 \, hours}{Z(p / nTorr) n_z} \cdot \left\{ \ln\left(\frac{2.5\gamma}{(\delta E / E)_{rf}} \right) - 1.4 \right\}^{-1} \cdot \left\{ \ln\left(\frac{1}{(\delta e / E)_{rf}} \right) - \frac{5}{8} \right\}^{-1} \qquad (4.22)$$

For an energy of 2 GeV, a pressure of 2 nTorr, Z = 7, n_z=2 and an energy acceptance of 1.2 %, the lifetime will be:

$$\tau_{Brems}(e) = \frac{9.30 \cdot 10^4 \, hours}{7 \cdot 2 \cdot 2} \cdot \{13.6 - 1.4\}^{-1} \cdot \{4.42 - 0.625\}^{-1} \qquad (4.23)$$

$$\tau_{Brems}(e) = 71.7 \, hours \qquad (4.24)$$

4.8.6 Touschek Lifetime

Within the bunches the electrons perform movements and according to this there exist a scattering between the stored electrons within one bunch. This scattering process has to be treated as Coulomb scattering. The lifetime of this called Touschek effect is given by:

$$\tau_{Tou} = \frac{8\pi\gamma^2 \sigma_x \sigma_y \sigma_l \varepsilon_{acc}^3}{r_e^2 c N_e} \cdot \frac{1}{D(\xi)} \qquad (4.25)$$

With the bunch volume $V_B = (4\pi)^{3/2}\sigma_x\sigma_y\sigma_l$ the Touschek lifetime is:

$$\tau_{Tou} = \frac{8\pi\gamma^2 V_B \varepsilon_{acc}^3}{(4\pi)^{3/2} r_e^2 c N_e} \cdot \frac{1}{D(\xi)} \qquad (4.26)$$

With the insertion of the constants Equation (4.26) changes to:

$$\tau_{Tou} = 6.57 \cdot 10^7\, hours \frac{(V_B / mm^3)\gamma^2 \varepsilon_{acc}^3}{N_e} \cdot \frac{1}{D(\xi)} \qquad (4.27)$$

Where:

σ_x =	average cross section in the horizontal direction
σ_y =	average cross section in the vertical direction
σ_l =	average cross section in the longitudinal direction
V_B =	bunch volume ($= (4\pi)^{3/2}\sigma_x\sigma_y\sigma_l$)
ε_{acc} =	energy acceptance of the accelerator which is normally the energy acceptance of the RF-system.
ξ =	$(\varepsilon_{acc} / \gamma\sigma_x')^2$ = normalized function
σ_x'=	$[\varepsilon_x\gamma_x + \eta'^2 (\sigma_E/E)^2]$ = maximum slope of the stored electrons
$D(\xi)$ =	normalized function
f =	filling factor
C =	circumference in meters

The function $D(\xi)$ is given in Figure (4.16) . Inserting the constant values into Equation (4.27), the Touschek lifetime will be:

$$\tau_{Tou} = 0.538 hours \frac{hf\,(E / GeV)^2 (\sigma_x / mm)(\sigma_y / mm)(\sigma_l / mm)\left[(\varepsilon_{acc} / \%\right]^3}{(I / A)(C / m) D(\xi)} \qquad (4.28)$$

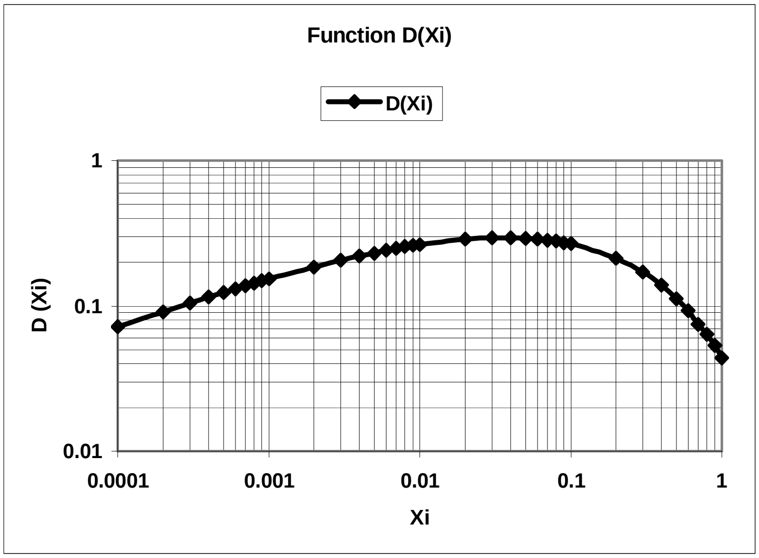

Figure 4.16: The function D(ξ) for the calculation of the Touschek life time

For the storage ring SESAME, we have the following data: E/GeV = 2, h = 200, C/m = 125, I/A = 0.4, f = 0.8, σ_x/mm = 0.465, $\sigma_{y/}$/mm = 0.040, σ_l/mm = 12, ε_x/mmmrad =16.8, $(\gamma_x)_{aver}$ = 1.5, $(\eta')_{max}$ = -0.4, σ_E/E = 0.0009, $(\sigma'_x)_{aver}$= 0.00015 rad, $(\xi)_{aver}$=0.0027 , ε_{acc} = 1.2 %, D(ξ) = 0.2.

With these values, the Touschek lifetime will be:

$$\tau_{Tou} = 13.8 \text{ hours}$$

4.8.7 Lifetime conclusions

The total lifetime of the stored beam is given by:

$$\frac{1}{\tau_{total}} = \frac{1}{\tau_{Coul}(N)} + \frac{1}{\tau_{Brems}(N)} + \frac{1}{\tau_{Coul}(e)} + \frac{1}{\tau_{Brems}(e)} + \frac{1}{\tau_{Tou}} \qquad (4.29)$$

The values of the total lifetime are summarized in Table (4.10) for the pressure 2 and 1 nTorr

Table 4.10: Lifetimes for the different interaction processes

	$\tau_{Coul}(N)$	$\tau_{Brems}(N)$	$\tau_{Coul}(e)$	$\tau_{Brems}(e)$	τ_{Tou}	τ_{Total}
P=2nTorr	22.6 h	27.4 h	967 h	71.7 h	13.8 h	5.9 h
P=1nTorr	45.2 h	54.8 h	1934 h	143.4 h	13.8 h	10 h

To get a lifetime in the range of 10 hours the pressure should be smaller than 1 nTorr.

References

[1] A. Ropert, "*Lattices and Emittances*" ,CERN Acc.School,Grenoble 1996,CERN 98-04.
[2] R.P.Walker, "*Synchrotron Radiation*" ,CERN Acc.School,Uni.of Jyvaskyla 1992,CERN 94-01.
[3] Philip J.Bryant & Kjell Johnsen, "*The Priciples of Circular Acc. and Storage Rings*" , *Chap. 6*.
[4] C. Bocchetta,"*Lifetime and beam quality*" ,*page252*,CERN Acc.Sch.,Grenoble1996,CERN 98-04.
[5] R. Walker,"*Insertion Devices: undolators and wigglers*" ,CERN Acc.Sch.,Grenoble1996,

CERN 98-04.
[6] H. Wiedemann, "*Particle Accelerator Physics1*", Chapter 7.
[7] Aharon Friedman & Eva Bozoki, "*Use of eigenvectors in understanding and correcting storage ring orbits*" , Nuclear Instruments and Methods in Physics Research A 344 (1994) 269-277.
[8] G.Guignard, "*Betatron coupling and related impact of radiation*", CERN Acc.Sch.,Rhodes 1993, CERN 95-06.